Advances in Science and Technology Research Journal

Advances in Science and Technology Research Journal 2023, 17(1), 23–34
https://doi.org/10.12913/22998624/157394
ISSN 2299-8624, License CC-BY 4.0

Received: 2022.11.07
Accepted: 2023.01.17
Published: 2023.02.01

Combined Effect of CrB_2 Micropowder and VN Nanopowder on the Strength and Wear Resistance of Fe–Cu–Ni–Sn Matrix Diamond Composites

Boranbay Ratov[1], Volodymyr Mechnik[2], Miroslaw Rucki[3*], Edwin Gevorkyan[4], Arturas Kilikevicius[3], Vasyl Kolodnitskyi[2], Zbigniew Siemiatkowski[4], Gulzada Umirova[1], Leszek Chalko[4], Jerzy Jozwik[5], Arailym Zhanggirkhanova[1], Volodymyr Chishkala[6], Dmytro Korostyshevskyi[2]

[1] Satbayev University, Institute of Geology and Oil and Gas K. Turysova, Department of Geophysics, Satpaev Str., 22, 050013, Almaty, Republic of Kazakhstan

[2] V. Bakul Institute for Superhard Materials of the NAS of Ukraine, Avtozavodska Str. 2, 04074 Kyiv, Ukraine

[3] Institute of Mechanical Science, Vilnius Gediminas Technical University, J. Basanaviciaus Str. 28, LT-03224 Vilnius, Lithuania

[4] Faculty of Mechanical Engineering, Kazimierz Pułaski University of Technology and Humanities, Stasieckiego Str. 54, 26-600 Radom, Poland

[5] Faculty of Mechanical Engineering, Lublin University of Technology, Nadbystrzycka Str. 36, 20-618 Lublin, Poland

[6] Department of Reactor Engineering Materials and Physical Technologies, V.N. Karazin Kharkiv National University, 4 Svobody Sq., 61022 Kharkiv, Ukraine

* Corresponding author's e-mail: m.rucki@uthrad.pl

ABSTRACT

The paper presents research results on the enhancement of diamond composites designed for tools application for mining industry, hard rocks cutting, able to withstand harsh conditions under heavy dynamical loads. In the present study, both CrB_2 micropowder and VN nanopowder additives were used in proportions up to 5 wt.% and 6 wt.%, respectively, together with the basic matrix composition of 51 wt.% Fe, 32 wt.% Cu, 9 wt.% Ni, and 8 wt.% Sn. Addition of both components, CrB_2 and VN, appeared to be advantageous in proportion of 2 wt.% and 4 wt.%, respectively. This composition exhibited the highest relative density of 0.9968, better than that without additives. Similarly, the highest values of compressive strength R_{cm} and flexural strength R_{bm} were reached for the composite with the same percentage of CrB_2 and VN. Compared to the composite with no addition of CrB_2 and VN, R_{cm} improved by almost 70%, while R_{bm} by 81%. Additionally, the abovementioned additives enhanced the ability of the matrix to prevent the diamond reinforcement from being torn out of the composite, which is very important under harsh working conditions of the cutting tools. The presence of CrB_2 micropowder and VN nanopowder promoted densification of the matrix and adhesion between the diamond grits and the Fe–Cu–Ni–Sn matrix.

Keywords: diamond composite, electroconsolidation, microstructure, adhesion, CrB_2, VN, wear resistance, cutting tools.

INTRODUCTION

Metal matrix composites (MMCs) reinforced with diamond exhibit high hardness and grinding ability and are widely used in various applications like drills for concrete and rock cutting, mining, tunneling, oil exploration, hydrological and geotechnical drilling [1–3]. In MMCs, diamond segments usually are attached to the cutting and grinding tools, e.g. drill bits, saw blades, or wire

saws [4]. It is important to note that in mining and rock technology, a single diamond particle of the cutting tool composite is not performing a cutting operation, but is rather acting as a sliding indenter causing confined crushing [5].

Apart from the rock mechanical properties [6], especially when transitioning between two distinct layers with different mechanical properties [7], the cutting performance and wear resistance of diamond-reinforced composites depends on the properties of a matrix primarily determined by its elemental composition [8], proportion of diamond grains added [9, 10], dimensions of the reinforcement [11], the strength and shape of diamond grits [12], and the additives that have effect on the composite microstructure [13]. In particular, Fe–Cu–Ni–Sn matrices are used for the diamond composites [14, 15], due to their high cutting characteristics and tribological properties useful for both soft soil and hard rocks in stationary and quarry conditions alike [16]. In particular, the following advantages of diamond Fe–Cu–Ni–Sn metal matrix composites can be named [17]:

- low cost of metal matrix components;
- relatively low temperature of a Cu–Sn system liquid phase appearance during sintering, contributing to the strength of diamond bits;
- the ability of cold pressing of metal matrix components in order to form tools of different shapes;
- improved environmental impact due to absence of toxic cobalt.

The liquid-state techniques for fabrication of metal matrix composites pose certain limits on the shape or size of the diamond reinforcement, while the powder metallurgy methods provide greater flexibility and ensure superb mechanical and thermal properties due to the uniform dispersion of the reinforcement [18]. The metal matrix composites reinforced with diamond grits are usually fabricated using pressure infiltration techniques and powder metallurgy [19], in particular, hot pressing methods (HP) [20]. Among other methods, hot isostatic pressing (HIP), high frequency induction heated sintering (HFJHS), and spark plasma sintering (SPS) can be named [21]. The fabrication method has direct impact on the phase and structure formation in the composite material [22, 23] thus influencing its further performance in working conditions [24].

Because the metal matrix has low hardness, its function is to hold the diamond grits in position and to ensure sufficient grain protrusion [25]. In the case of tool operation, it is crucial that the matrix have high retention properties to ensure sufficient retention of the diamond particles to prevent them from falling out, pressing in or turning during cutting [26]. This condition guarantees the appropriate exposing of new diamond particles out of the worn tool, with new, sharp cutting edges. However, under heavy unstable contact loads and elevated temperatures, irreversible structural changes may occur in the matrix, decreasing its modulus and accelerating its wear. It is suggested that the pullout and fracture of reinforcing particles could be the main tool wear mechanisms, perhaps due to high working temperature [27]. Moreover, another possible wear mechanism is the dulling of diamond grits resulting in a worsened cutting performance, which can be avoided by proper adjusting of the metal matrix hardness [28]. Additionally, graphitization of the diamond bits substantially reduces its serving time [29,30]. Thus, to enhance the cutting tool, it is necessary to add some substances that would strengthen the matrix on the one hand, and improve adhesion between the matrix and the diamond reinforcement.

Among others, CrB_2 additive was found useful as a strengthening component of the diamond-reinforced metal matrix composites [31, 32]. It was demonstrated that addition of 2 wt.% of CrB_2 to the Fe–Cu–Ni–Sn matrix, together with relevant optimization of the sintering conditions, enhanced retention of the diamond grits in the matrix and provided decarburization bonding the non-diamond carbon to the compounds like Cr_3C_2, Cr_7C_3, $Cr_{1.65}Fe_{0.35}B_{0.96}$ [33]. Moreover, experiments showed that increase of the CrB_2 content up to 8 wt.% in the matrix of 51 wt.% Fe – 32 wt.% Cu – 9 wt.% Ni – 8 wt.% Sn increased both hardness and modulus [34].

In turn, addition of vanadium nitride (VN) to the Fe–Cu matrix system improved its flexural strength and hardness by 25% and 30%, respectively, presumably due to the better adhesion between matrix and diamond grits [35]. Also the Fe–Cu–Ni matrix increased almost twice its compressive and flexural strength and decreased wear rate after VN nanopowder was added [36]. These results indicated that combination of both CrB_2 and VN additives in the diamond-reinforced Fe–Cu–Ni–Sn matrix would improve the properties

of the composite from the perspective of cutting tools destined for mining and rock cutting.

In this respect, the present work is aimed to investigate the effect of combined CrB_2 and VN additives on the diamond composite with the matrix of 51 wt.% Fe – 32 wt.% Cu – 9 wt.% Ni – 8 wt.% Sn. The objective was to find out the most advantageous proportion of the components in terms of mechanical characteristics, such as hardness H, elastic modulus E, resistance to plastic deformation H^3/E^2 [37], index of tolerance to abrasion damage $1/(E^2H)$ [38], compressive strength, and flexural strength. Moreover, adhesion to the diamond grits was taken into consideration as an important enhancing factor for this application.

MATERIALS AND METHODS

The fabrication method was electroconsolidation, which belongs to the group of Spark Plasma Sintering (SPS) [39] or Field Activated Sintering Technique (FAST) [40]. For this method, specimens of pure matrices were prepared sintering the powder blends of iron (Fe), copper (Cu), nickel (Ni), tin (Sn), chromium diboride (CrB_2), and vanadium nitride (VN), while to obtain the diamond composite specimens, diamond powder was added. The particle dimensions provided by the respective delivering companies of the components are specified in the Table 1.

First sample of the specimens prepared for different tests consisted of pure Fe–Cu–Ni–Sn matrices with no additions of chromium diboride, vanadium nitride or diamond. Next samples, #2 to #7, were sintered out of Fe–Cu–Ni–Sn–CrB_2–VN components with various combinations of CrB_2 and VN proportions. Samples #8 to #11 kept similar proportions of CrB_2 and VN but with addition of 6.25 wt.% of diamond powder. And sample #12 contained 5 wt.% of each CrB_2 and VN compound, as well as diamond powder. Proportions of the components in each sample of specimens are shown in Table 2.

Based on the previous experience, homogenous powder blend for sample #1 was prepared as follows. First, Sn and Ni powders in respective amounts were mixed together in the alcohol environment. Then the appropriate amount of Cu powder was added and mixed until the uniform

Table 1. Powders used in the experiments

Powder	Particle dimensions (μm)	Delivering company	City, country
Fe	25 ± 10	Powder Metallurgy Enterprise	Zaporizhzha, Ukraine
Cu	20 ± 9	Powder Metallurgy Enterprise	Zaporizhzha, Ukraine
Ni	15 ± 8	Powder Metallurgy Enterprise	Zaporizhzha, Ukraine
Sn	15 ± 8	Powder Metallurgy Enterprise	Zaporizhzha, Ukraine
CrB_2 70.62 % of Cr and 29.30 % of B	7 ± 6	OOO Synthex-Product	Moscow, Russia
VN	0.5 ± 0.4	ONYXMET	Olsztyn, Poland
Diamond powder	0.5 ± 0.36	De Beers	South Africa

Table 2. Proportions of the components in each sample of specimens

Sample	$C_{diamond}$	Fe	Cu	Ni	Sn	CrB_2	VN
1	–	51	32	9	8	–	–
2	–	47.94	30.08	8.46	7.52	2	4
3	–	49.47	31.04	8.73	7.76	1	2
4	–	45.90	28.80	8.10	7.20	4	6
5	–	46.92	29.44	8.28	7.36	2	6
6	–	46.92	29.44	8.28	7.36	4	4
7	–	49.90	28.80	8.10	7.20	4	5
8	6.25	47.8125	30.0	8.4375	7.5	–	–
9	6.25	44.7525	28.08	7.8975	7.02	2	4
10	6.25	46.2825	29.04	8.1675	7.26	1	2
11	6.25	42.7125	26.80	7.5375	6.7	4	6
12	6.24	42.7125	26.80	7.5375	6.7	5	5

blend was reached. And next, Fe powder was added and mixed in the similar way.

The samples #2 to #7 were prepared using the following procedure. First, CrB_2 and VN powders in respective amounts were mixed together in the alcohol environment. Next, respective Sn, Ni, Cu, Fe powders were subsequently added and mixed in the way described above.

To prepare the samples of the diamond composite #8 without CrB_2 and VN additions, the powder blend #1 was prepared first. Then the diamond powder moistened with glycerin was added in a batch of 6.25 wt.% and mixed together in the alcohol environment until the uniform blend was reached. Similarly, samples #9 to #12 were prepared according to the procedures for #2 – #4, and then the diamond powder was added.

The abovementioned powder blends underwent sintering process in the graphite molds, using a modified electroconsolidation method, which has been described in detail elsewhere [41]. Graphite molds were lubricated with boron nitride to prevent their interaction with sintered specimens. The process parameters were determined based on the results of preliminary studies [22]. The samples of 10 mm diameter and 5 mm thickness, were sintered in vacuum of 0.1 Pa under alternating current of 5000 A, voltage 5 V. The heating rate was 300 °C/min, mechanical pressure 30 MPa was applied for 3 minutes. Sintering temperatures were from 20 °C up to 1000 °C. It is worth noting that the temperature and time of sintering are below the recently reported 1550 °C and 5 min [42], which indicates substantial savings and lays in accordance with optimisation of the sintering method named among the main measures to improve diamond composites [43].

The sintered specimens were grinded to obtain cylinders of 9.62 mm diameter and 4.84 thickness. Before the microstructural and mechanical tests, the surfaces of specimens were polished with a diamond paste of 1 μm particle dimensions and with colloid solution containing silicon oxide particles of 0.04 μm size to obtain a mirror-like surface. For the compressive strength tests with displacement rate 1 μm/s, specimens were cut in form of the bars with cross section 2×2 mm.

To determine the relative density ρ, the following equation was applied:

$$\rho = \frac{\rho_h}{\rho_t} \tag{1}$$

where: ρ_h – the hydrostatic density (g/cm^3);
ρ_t – the true density (g/cm^3).

The true density ρ_t was measured using helium pycnometry system AccuPyc 1340 made by Micromeritics (Norcross, GA, US). The hydrostatic density ρ_h was calculated from the following equation:

$$\rho_h = \rho_{H2O} \frac{M_1}{M_2 - M_3} \tag{2}$$

where: ρ_{H2O} – the density of water (≈1 g/cm^3);
M_1 – the mass of the composite in air;
M_2 – the mass of the composite covered by the protective film (vaseline) in air;
M_3 – the mass of the composite covered by the protective film in water. The mass was measured using laboratory scales with sensitivity 0.001 g.

Microstructure, morphology, and elemental composition were analyzed using scanning electron microscope (SEM) Mira 3 LMU delivered by TESCAN (Czech Republic). Its resolution was 1.2 nm, with application of energy dispersion microanalyzer OXFORD X-MAX 80 mm^2. The measurement uncertainty for heavy metals was 0.01 wt.%, while for light metals it was 0.10 wt.%. During analysis of the sample surface, the accelerating voltage was 30 kV, Cu$K\alpha$ radiation, λ_{Cu} = 0.1542 nm.

Micromechanical hardness tests and measurement of elastic modulus E were performed with Nano Indenter G200 made by Agilent Technologies (USA). It was equipped with the pyramidal sharp-tip Berkovich indenter, and the nanoindentation depth was 200 nm. Nanohardness H and elastic modulus E were determined using Oliver–Pharr method [44]. In this method, the diamond tip and the sample are modeled as two contacting bodies, and direct measurement of stiffness S and projected area of contact A_c allows for the sample elasticity modulus E to be evaluated. At least 10 indentations under the load ±20–24 mN were made on the surface of each tested specimen, distanced from one another by10–15 μm, to calculate the arithmetic mean value. The indentation depth measurement was performed with accuracy of ±0.04 nm.

The compressive strength R_{cm} was measured with a Landmark MTS 870 Dual Column machine produced by MTS company (Eden Prairie, MN, USA) at 1 μm/s displacement rate. The three-point flexural test was used to determine the flexural strength R_{bm}. The test was performed using Instron

3344 testing device (INSTRON Ltd., Norwood, MA, USA) at the displacement rate of 1 μm/s. The process was registered by 10,000 pictures per second, using a Photron FASTKAM Mini UX100 M1 camera (Photron USA, Inc., San Diego, CA).

RESULTS AND DISCUSSION

Morphology of the initial powders

In Figure 1, there are shown SEM images of the diamond particles (1a), chromium diboride (1b) and vanadium nitride (1c) used as the initial powders for the subsequent sintering. The diamond particles of dimensions 0.5 ± 0.36 μm exhibit well-developed facets of various simple shapes. On the surfaces of the particles seen in Fig. 1a, no defects are distinguishable, such as cracks, chips, or cavities.

Chromium diboride particles presented in Fig. 1b have average size of 4–6 μm and mainly irregular shape with developed surface. Some larger particles were found in the powder, which perhaps were agglomerated from the small particles. Vanadium nitride VN powder in Fig. 1c had particle dimensions in wider range, from 0.1 up to 0.7 μm. Two sorts of agglomerates can be distinguished. The first order agglomerates exhibit spherical shape of dimensions ca. 0.1 μm. The second order agglomerates have rather polygonal shape with skewed angles, but also rounded ones. Mainly their dimensions are about 0.3 μm, but single agglomerates reach up to 1 μm. Presumably, agglomeration takes place through clumping of smaller VN particles together. It should be noted, however, that amount of the large agglomerates between 0.3 and 0.7 μm is relatively small, below 5%.

The abovementioned morphological features may have certain effect on the microstructure, and, hence, performance of the sintered samples.

Microstructural features of the sintered specimens

Effect of the additions on the MMC's sintering ability and, thus, on the final structure is seen in the diagram of the relative density ρ. Figure 2

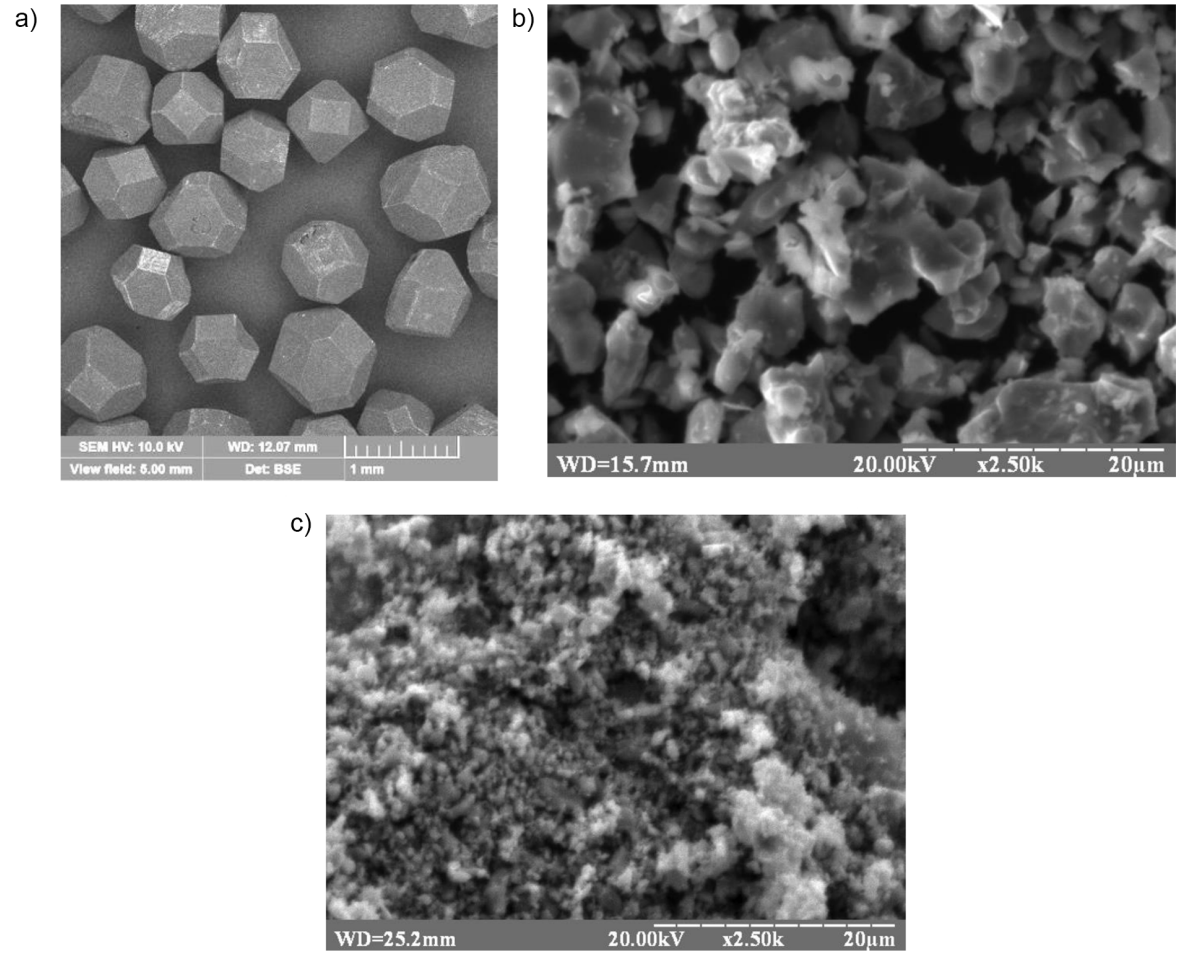

Fig. 1. SEM images of the initial powders: a) diamond particles, b) chromium diboride, and c) vanadium nitride

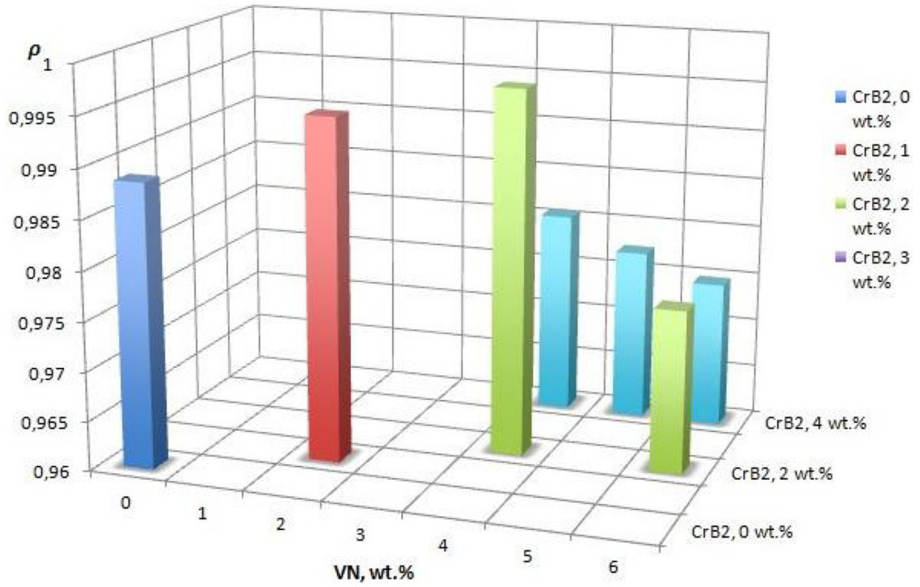

Fig. 2. Diagram of relative density ρ after addition of different proportions VN and CrB_2 to the matrix 51 wt.% Fe – 32 wt.% Cu – 9 wt.% Ni – 8 wt.%

shows results for different percentage of the VN and CrB_2 by mass. It demonstrates that the density of the matrix without these additions was ρ = 0.9886, and increased after some amounts of vanadium nitride and chromium diboride were added. The maximal relative density ρ = 0.9968 was obtained for the composition with 2 wt.% of CrB_2 and 4 wt.% of VN. Further increase of both components resulted with drastic decrease of the relative density down to ρ = 0.9748 after addition of 4 wt.% of CrB_2 and 6 wt.% of VN.

These results are conditioned by the dispersity of the initial powders, discussed in the previous section. In particular, formation of agglomerates during the mixing procedure had significant effect, as well as their separation during the sintering. As a result, micropores must have been formed, since the sintering temperature of VN and CrB_2 additives is much higher that that of other MMC's components and their agglomerations can be sintered only partially. From the application perspective, porosity is disadvantageous due to hardness reduction and decrease of the related mechanical properties and performance.

Apart from porosity and relative density, the additives had effect on the contact between the matrix and diamond reinforcement. Figure 3 presents example of the SEM images obtained

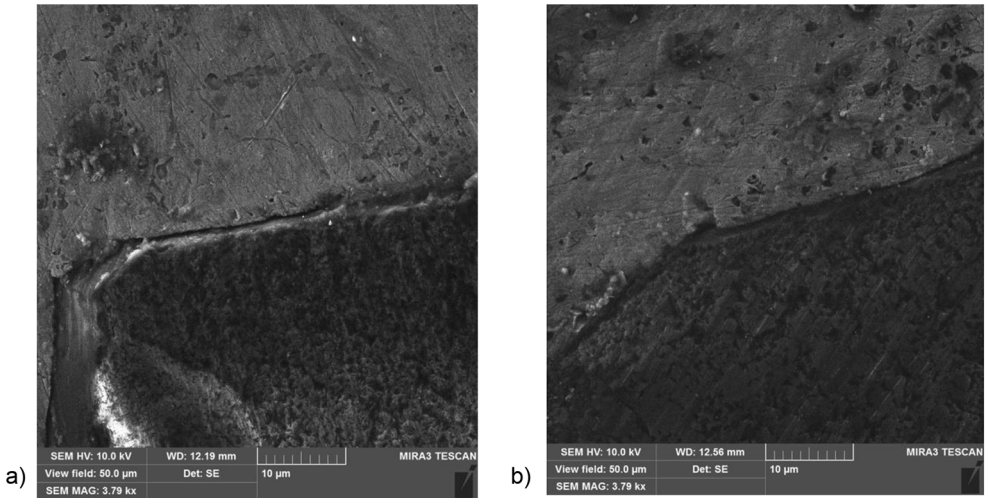

Fig. 3. SEM images of the contact area between the matrix and the diamond grits (composition contrast): a) sintered sample #8 without CrB_2 and VN additions, b) sample #9 with 2 wt.% CrB_2 and 4 wt.% VN

for the samples #8 and #9. Their compositions were 6.25 wt.% $C_{diamond}$ – (51 wt.% Fe–32 wt.% Cu–9 wt.% Ni–8 wt.% Sn) for the sample #8, and 6.25 wt.% $C_{diamond}$ – (47.75 wt.% Fe–28.08 wt.% Cu–7.89 wt.% Ni–7.02 wt.% Sn–2 wt.% CrB_2–4 wt.% VN) for the sample #9. These images illustrate peculiarities of the contact area between the matrix and the diamond grits used as reinforcement. Especially from the cutting tool application perspective, this contact area is crucial for the performance and especially for wear resistance of the composite.

In general, structures of the samples #8 and #9 are quite similar, while the #9 looks more dispersive. In sample #8 without CrB_2 and VN additions shown in Fig. 3a, contact between the diamond grit and the matrix is untied with distinguishable discontinuities and gaps. These features indicate weakness of the diamond fixation in the matrix. Obviously, under dynamic loads during the work of the cutting tools, the contact area could be easily destroyed which reduce ability of the matrix to keep the diamond grits in place. After addition of 2 wt.% CrB_2 and 4 wt.% VN, the structure of the metal matrix becomes more dispersive and the contact with the diamond surface is more tight, with no discontinuities seen in the sample #9, Fig. 3b. This simple observation indicates that micropowder CrB_2 and nanopowder VN added to the Fe–Cu–Ni–Sn matrix enhanced retention of the diamond reinforcement. However, the improvement was seen only for small percentage of these additions, their further increase resulted with appearance of defects in form of discontinuities, cavities, etc., indicating worsened performance of the diamond-reinforced metal matrix composite.

Mechanical properties

It was demonstrated previously that decrease of both modulus E and nanohardness H not necessarily resulted with worsened performance, if the respective indexes H/E, H^3/E^2, and $1/(E^2/H)$ increased, accordingly [32]. Table 3 presents the values of nanohardness H, modulus E, elastic strain to failure ratio H/E, resistance to plastic deformation index H^3/E^2, and index of tolerance to abrasion damage $1/(E^2H)$ for the matrices 51 wt.% Fe – 32 wt.% Cu – 9 wt.% Ni – 8 wt.% Sn with different percentages of the micropowder CrB_2 and nanopowder VN added.

The experimental results demonstrated that the metal matrix without any additions of CrB_2 and VN exhibited the highest modulus E, but the lowest hardness and all indexes H/E, H^3/E^2, $1/(E^2H)$. Any amount of CrB_2 and VN added to the matrix improved its mechanical characteristics. For instance, the smallest percentage of additives in sample #3 resulted with more than 22% increased hardness and almost three times higher resistance to plastic deformation index H^3/E^2. Decrease of the modulus E caused by the additions CrB_2 and VN took place due to the microstructure refinement. It was suggested elsewhere [45] that this phenomenon was promoted by the phase transformation α→γ→α. Subsequent increase of the indexes H/E, H^3/E^2, $1/(E^2H)$ is advantageous for the MMCs reinforced with diamonds for tool applications.

Particularly advantageous appeared to be additive proportion in sample #2 with 2 wt.% CrB_2 and 4 wt.% VN. It exhibited the highest value of hardness and of all indexes H/E, H^3/E^2, $1/(E^2H)$. Noteworthy, the same proportion ensured the highest density (Fig. 2) and the best contact with diamond grits (Fig. 3b). Presumably, this proportion provided the best conditions for the sintering process providing the most dense and homogenous structure.

Further increase of the amount of CrB_2 and VN added to the matrix resulted with the agglomeration of nano-VN particles and subsequent

Table 3. Mechanical properties of the matrices 51Fe–32Cu–9Ni–8Sn with different percentages of additions CrB_2 and VN

Sample	CrB_2, wt.%	VN, wt.%	H, GPa	E, GPa	H/E	H^3/E^2, MPa	$1/(E^2H)$, GPa^{-3} ($\times10^{-5}$)
#1	–	–	6.1 ± 0.9	172 ± 9	0.035	7.672	0.554
#3	1	2	7.5 ± 07	139 ± 8	0.054	21.842	0.690
#2	2	4	8.2 ± 1.1	124 ± 11	0.066	35.902	0.793
#6	4	4	8.1 ± 0.6	130 ± 7	0.062	31.446	0.731
#7	4	5	7.4 ± 0.9	134 ± 12	0.055	22.568	0.752
#5	2	6	7.0 ± 1.0	140 ± 10	0.050	17.508	0.729
#4	4	6	6.5 ± 0.8	154 ± 9	0.042	11.580	0.649

Table 4. Strength of the matrices 51Fe–32Cu–9Ni–8Sn with different percentages of additions CrB_2 and VN

Sample	CrB_2 wt.%	VN, wt.%	R_{bm}, MPa	R_{cm}, MPa
#1	–	–	740 ± 20	950 ± 70
#3	1	2	1140 ± 60	1510 ± 90
#2	2	4	1250 ± 50	1720 ± 90
#6	4	4	1190 ± 70	1640 ± 80
#7	4	5	1060 ± 40	1420 ± 10
#5	2	6	910 ± 30	1240 ± 80
#4	4	6	840 ± 40	1020 ± 60

micropore formation around the agglomerates. Thus, the addition of CrB_2 above 2 wt.% and VN above 4 wt.% appeared to be disadvantageous in terms of wear resistance and durability in a rock cutting tools application.

Results of the strength tests, including compressive strength R_{cm} and flexural strength R_{bm}, are shown in Table 4. Again, the metal matrix without any additions of CrB_2 and VN exhibited the lowest strength, so that even minimal amounts added improved both flexural and compressive strength. The smallest percentage of additives in sample #3 increased strength R_{cm} by almost 60% and R_{bm} by 54% in average.

Proportion of additives in sample #2 with 2 wt.% CrB_2 and 4 wt.% VN had particularly advantageous effect on the strength of the metal matrix. It exhibited the highest values of flexural strength R_{bm} = 1250 MPa and compressive strength R_{cm} = 1720 MPa, which corresponds with improvement by 69% and 81%, respectively, compared to sample #1. Further increase of the concentration of CrB_2 and VN in the matrix 51 wt.% Fe – 32 wt.% Cu – 9 wt.% Ni – 8 wt.% resulted with gradual weakening of the composite. However, the lowest strength of sample #4 with 4 wt.% CrB_2 and 6 wt.% VN was still higher than that of sample #1 without additions.

Comparison of the results presented in Figure 2 and in Tables 3 and 4 reveals the similar trend. Namely, addition of micro CrB_2 and nano VN powders improved densification and increased hardness and wear resistance with the best characteristics for 2 wt.% CrB_2 and 4 wt.% VN proportion. Larger amounts of the additives appeared to be disadvantageous from the perspective of cutting tools application. Other reports confirmed that the most advantageous percentage of CrB_2 additive in Fe–Cu–Ni–Sn was 2 wt.% [34]. As for vanadium nitride, 4 wt.% of VN provided maximal values of flexural strength R_{bm} = 1110 MPa and compressive strength R_{cm} = 1410 MPa, while maximum values of nanohardness H = 7.8 GPa, ratio H/E = 0.0366, and index H^3/E^2 = 10.46 MPa were reached at proportion of 8 wt.% of nano-VN reinforcement [17]. Combined addition of both substanced in proportion of 2 wt.% CrB_2 and 4 wt.% VN provided much better results.

Analysis of fracture surface

It was found useful also to analyze the fracture surface in order to observe some peculiarities of the structural modifications with combined addition of chromium diboride and vanadium nitride to the Fe–Cu–Ni–Sn metal matrix. Especially in terms of retention of diamond reinforcing grits in the matrix, fractography appears to provide additional evidence. Examples of the SEM images of fracture surfaces obtained after impact at 20 °C are presented in Figure 4. To illustrate the strength of the contact between the diamond and the matrix, samples #8, #9, and #11 were chosen.

The composition of the samples shown in Figure 4 was as follows:

- #8: 6.25 wt.% $C_{diamond}$ – (51 wt.% Fe–32 wt.% Cu–9 wt.% Ni–8 wt.% Sn),
- #9: 6.25 wt.% $C_{diamond}$ – (47.75 wt.% Fe–28.08 wt.% Cu–7.89 wt.% Ni–7.02 wt.% Sn–2 wt.% CrB_2–4 wt.% VN),
- and #11: 6.25 wt.% $C_{diamond}$ – (42.71 wt.% Fe–26.80 wt.% Cu–7.53 wt.% Ni–6.7 wt.% Sn–4 wt.% CrB_2–6 wt.% VN.

It can be seen in Fig. 4a that the composite sample #8 withstanding impact at room temperature exhibited fracture along the body of its metal matrix. The surfaces of the diamond grit remained undamaged since the strength of the diamond itself was much higher than that of its adhesion to the matrix. Areas of ductile pitting fracture and individual facets of brittle chipping reveal combined ductile-brittle fracture character. Moreover, some micropores can be seen together with the irregularly shaped tear areas with significant deformation. Added CrB_2 and VN in sample #9 shown in Fig. 4b contributed to the formation of more fine-grained, loose structure of the metal matrix. Moreover, the surface of the diamond grits appears to be damaged, exposing microsteps after the part of upper microlayer was chipped away. It can be assumed that the bond between the diamond grit and the matrix was stronger than the diamond itself, causing damage of the latter instead of being torn of its surface.

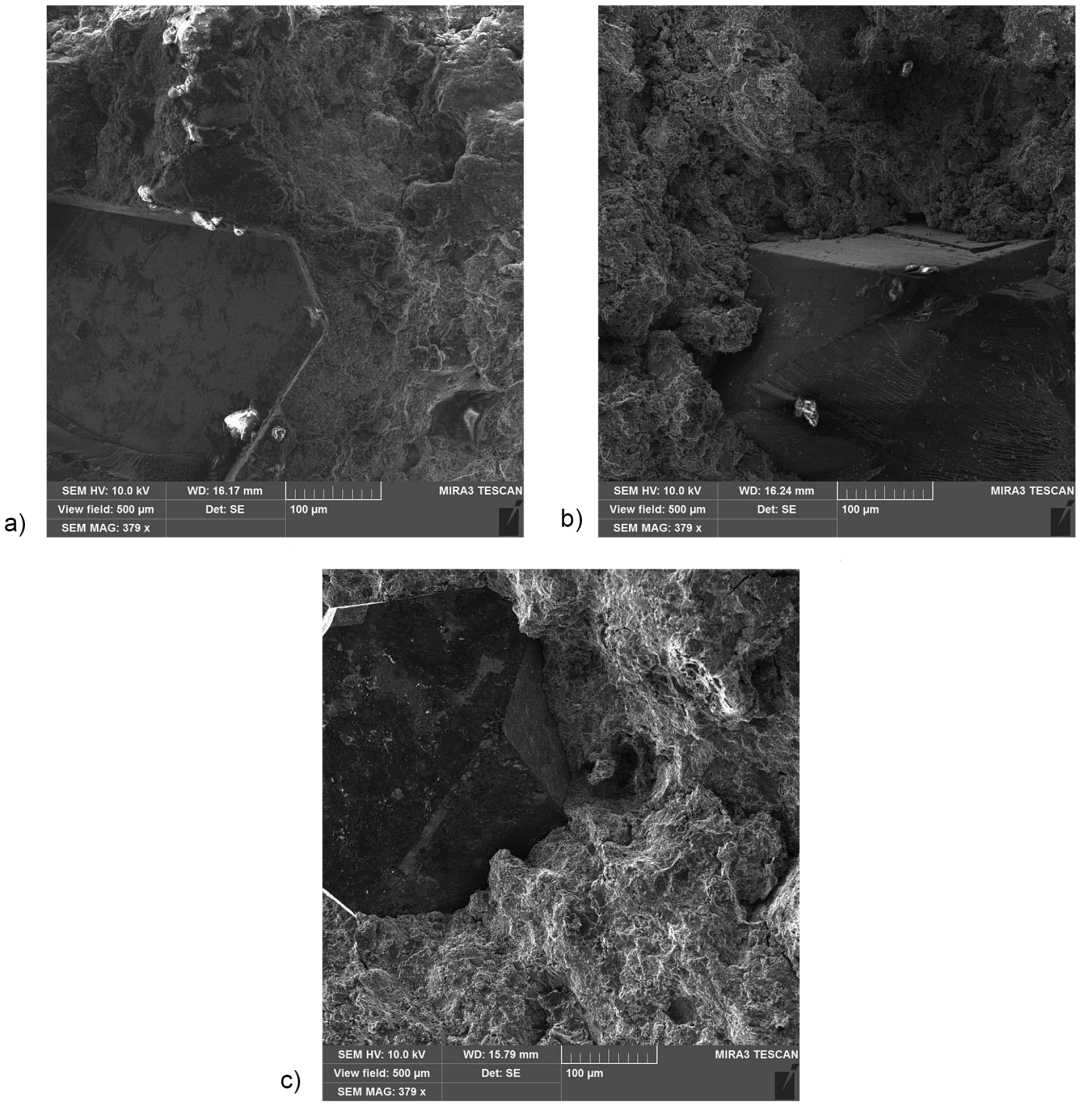

Fig. 4. SEM images of the fracture surfaces close to the diamond grits: a) sintered sample #8 without CrB_2 and VN additions, b) sample #9 with 2 wt.% CrB_2 and 4 wt.% VN, c) sample #11 with 4 wt.% CrB_2 and 6 wt.% VN

Further increase of the CrB_2 and VN powders proportion caused weakening of the diamond-matrix bonds. On the surface of the diamond exposed after fracture, numerous strips of the matrix material can be seen in Fig. 4c. Thus, in the sample #11 with higher concentration of both CrB_2 and VN, adhesion between the diamond and the matrix material is stronger than the bonds inside the matrix, but weaker than that of diamond. Additionally, microcracks in the matrix can be seen in the perpendicular direction to the main fracture plane.

CONCLUSIONS

From the presented results it can be concluded that the proposed, modified FAST method provided fine microstructure and high relative density due to the high densification rate of 300 °C/min and short sintering time of 3 minutes. It was found that the combined addition of both CrB_2 and VN promoted enhancement of the matrix composed of 51 wt.% Fe – 32 wt.% Cu – 9 wt.% Ni – 8 wt.% Sn. The concentration of additives 2 wt.% CrB_2 and 4 wt.% VN provided the highest hardness of 8.2 ± 1.1 MPa, wear resistance indexes, and strength. The values of flexural strength R_{bm} = 1250 MPa and compressive strength R_{cm} = 1720 MPa exhibited improvement by 69% and 81%, respectively, compared to that of the matrix without CrB_2 and VN additions.

Presumably, the proportion 2 wt.% CrB_2 and 4 wt.% VN provided the best sintering ability of the powder mixture due to the morphology of the mixed powders. Larger amounts of the chromium diboride and vanadium nitride promoted

agglomeration of the particles with subsequent micropores formation around agglomerates, preventing from full densification. As a result, concentrations above 2 wt.% CrB_2 and 4 wt.% VN reduced relative density and the mechanical properties of the matrices. However, the characteristics remained still better than the ones of matrices without addition of CrB_2 and VN.

Important feature of the examined MMCs was better fixation of diamond grains and enhanced adhesion between the matrix and diamond reinforcement due to the improved sintering ability of the powders. Analysis of SEM images, especially that of fracture surfaces, proved the proportion 2 wt.% CrB_2 and 4 wt.% VN to be the most advantageous in terms of retention of the diamond reinforcement in the metal matrix.

Among the tested compositions, the one with 6.25 wt.% $C_{diamond}$ – (47.75 wt.% Fe–28.08 wt.% Cu–7.89 wt.% Ni–7.02 wt.% Sn–2 wt.% CrB_2–4 wt.% VN) appeared to be the most promising and worthy further investigation. Its fabrication with the modified electroconsolidation method is worthy attention, too, due to the energy and time savings.

Acknowledgments

The publication was financed from the funds of the Polish Ministry of Education and Science as part of the program ”Social Responsibility of Science/Excellent Science”, support for Scientific Conferences „Synergy of Science and Industry”, Challenges of the 21st Century, Science – Industry – Business. The research has been performed within the framework of state funded research topics in accordance with the coordination plans of the Ministry of Education and Science of Ukraine (state registration number 0120 U100105), and co-funded by the Science Committee of the Ministry of Education and Science of the Republic of Kazakhstan, Grant No. AP14869271.

REFERENCES

1. Sun Y., Zhang C., He L., Meng Q., Liu B.-C., Gao K., Wu J. Enhanced bending strength and thermal conductivity in diamond/Al composites with B4C coating. Scientific Reports 2018; 8: 11104. https://doi.org/10.1038/s41598-018-29510-7
2. Ivasiv V., Yurych A., Zabolotnyi S., Yurych L., Bui V., Ivasiv O. Determining the influ- ence of the condition of rockdestroying tools on the rock cutting force. Eastern-European Journal of Enterprise Technologies 2020; 1(103): 15–20.
3. Ratov B.T., Fedorov B.V., Kuttybaev A.E., Sarbopeeva M.D., Borash B.R. Drilling tools with compound cutting structure for hydrological and geotechnical drilling. MIAB. Mining Inf. Anal. Bull. 2022; (9): 42–59. https://doi.org/10.25018/0236_1493_2022_9_0_42 [In Russian].
4. Malevich N., Müller C.H., Dreier J., Kansteiner M., Biermann D., De Pinho Ferreira M., Tillmann W. Experimental and statistical analysis of the wear of diamond impregnated tools. Wear 2021; 468–469: 203574. https://doi.org/10.1016/j.wear.2020.203574
5. Brook B. Principles of diamond tool technology for sawing rock. International Journal of Rock Mechanics and Mining Sciences 2002; 39(1): 41–58. https://doi.org/10.1016/S1365-1609(02)00007-2
6. Menezes P.L. Influence of rock mechanical properties and rake angle on the formation of rock fragments during cutting operation. The International Journal of Advanced Manufacturing Technology 2017; 90: 127–139.
7. Aribowo A.G., Wildemans R., Detournay E.,. van de Wouw N. Drag bit/rock interface laws for the transition between two layers. International Journal of Rock Mechanics and Mining Sciences 2022; 150; 104980. https://doi.org/10.1016/j.ijrmms.2021.104980
8. Hu H., Chen W., Deng C., Yang J. Effect of matrix composition on the performance of Fe-based diamond bits for reinforced concrete structure drilling. Int. J.Refract. Met. Hard Mater. 2021; 95: 105419.
9. Vynohradova O.P., Zakora A.P., Shul'zhenko A.A., Gargin V.G., Sokolov A.N., Efrosinin D.V., Zakora I.A. Comparative Evaluation of the Performance of Drill Bits with a Diamond-Containing Matrix and Inserts Made of Diamond-Containing Composites. J. Superhard Mater. 2022; 44: 57–61. https://doi.org/10.3103/S1063457622010099
10. He T., Zhang S., Kong X., Wu J., Liu L., Wu D., Su Z. Influence of diamond parameters on microstructure and properties of copper-based diamond composites manufactured by Fused Deposition Modeling and Sintering (FDMS). Journal of Alloys and Compounds 2023; 931: 167492. https://doi.org/10.1016/j.jallcom.2022.167492
11. Saba F., Zhang F., Liu S., Liu T. Reinforcement size dependence of mechanical properties and strengthening mechanisms in diamond reinforced titanium metal matrix composites. Composites Part B: Engineering 2019; 167: 7–19. https://doi.org/10.1016/j.compositesb.2018.12.014
12. Huang Y., Zhang F., Zha M., Zhu M., Zhou Y., Tang H., Xie D. Mechanical properties and tribological

behavior of Fe/nano-diamond composite prepared by hot-press sintering. Int. J. Refract. Met. Hard Mater. 2021; 95: 105412

13. Su Z., Zhang S., Wu J. Effect of nickel-plated graphite on microstructure and properties of matrix for Fe-based diamond tools. Transactions of Nonferrous Metals Society of China 2022: 32(5): 1575–1588. https://doi.org/10.1016/S1003-6326(22)65894-1
14. Li M., Sun Y., Meng Q., Wu H., Gao K., Liu B. Fabrication of Fe-based diamond composites by pressureless infiltration. Materials 2016; 9: 1006.
15. Borowiecka-Jamrozek J.M., Konstanty J., Lachowski J. The application of a ball-milled Fe–Cu–Ni powder mixture to fabricate sintered diamond tools. Arch. Found. Eng. 2018; 18(1): 5–8.
16. Cygan-Bączek E., Wyżga P., Cygan S., Bała P., Romański A. Improvement in Hardness and Wear Behaviour of Iron-Based Mn–Cu–Sn Matrix for Sintered Diamond Tools by Dispersion Strengthening. Materials 2021: 14: 1774. https://doi.org/10.3390/ma14071774
17. Mamalis A., Mechnik V., Morozow D., Ratov B., Kolodnitskyi V., Samociuk W., Bondarenko N. Properties of Cutting Tool Composite Material Diamond–(Fe–Ni–Cu–Sn) Reinforced with Nano-VN. Machines 2022; 10(6): 410. https://doi.org/10.3390/machines10060410
18. Kim D.-Y., Choi H.-J. Recent Developments towards Commercialization of Metal Matrix Composites. Materials 2020; 13(12): 2828. https://doi.org/10.3390/ma13122828
19. Yin S., Xie Y., Cizek J., Ekoi E.J., Hussain T., Dowling D.P., Lupoi R. Advanced diamond-reinforced metal matrix composites via cold spray: Properties and deposition mechanism. Composites Part B: Engineering 2017; 113: 44–54. https://doi.org/10.1016/j.compositesb.2017.01.009
20. Han P., Lu X., Li W., Zou W. Influence of Ni, Fe and Co on the microstructure and properties of 75% Cu–25% Sn alloy in hot pressing. Vacuum 2018; 154: 359–365, https://doi.org/10.1016/j.vacuum.2018.05.016
21. Konstanty J. Powder Metallurgy Diamond Tools. Elsevier, 2005.
22. Gevorkyan E., Mechnik V., Bondarenko N., Vovk R., Lytovchenko S., Chishkala V., Melnik O. Peculiarities of obtaining diamond–(Fe–Cu–Ni–Sn) hot pressing. Functional Materials 2017; 24: 31–45.
23. Kolodnits'kyi V.M., Bagirov O.E. On the structure formation of diamond-containing composites used in drilling and stone-working tools (A review). J. Superhard Mater. 2017; 39(1): 1–17.
24. Li S., Han Z., Meng Q., Zhao X., Cao X., Liu B. Effect of WC Nanoparticles on the Microstructure and Properties of WC-Bronze-Ni-Mn Based Diamond Composites. Applied Sciences 2018; 8(9): 1501. https://doi.org/10.3390/app8091501
25. Denkena B., Grove T., Bremer I., Behrens L. Design of bronze-bonded grinding wheel properties. CIRP Ann. - Manuf. Technol. 2016; 65: 333–336.
26. Novak P., Belezze T., Cabibbo M., Gamsjager E., Wiessner M., Rajnovic D., Jaworska L., Hanus P., Shishkin A., Goel G., Goel S. Solurions of critical raw materials issues regarding iron-based alloys. Materials 2021; 14: 899.
27. Li M., Jiang X., Chen Y., Yang X. Hole surface morphology and tool wear mechanisms during cutting 3D carbon/carbon composites using diamond core drill. Ceramics International 2022, in Press, https://doi.org/10.1016/j.ceramint.2022.10.128
28. Sagradyan A.I., Agbalyan S.G., Martirosyan A.M., Ordyan N.A., Pogosyan H.V. Extending life of diamond tools for machining nonmetallic materials. J. Superhard Mater. 2018; 40(3): 216–221.
29. Liu C., Zhou F., Man Z., Liu Y. Analysis of drilling failure in soft and hard sandwiching of coal seam. Engineering Failure Analysis 2016; 59: 544–553. https://doi.org/10.1016/j.engfailanal.2015.10.022
30. Xiang J., Xie L., Gao F., Yi J., Pang S., Wang X. Diamond tools wear in drilling of SiCp/Al matrix composites containing Copper. Ceram. Int. 2018; 44: 5341–5351.
31. Ratov, B.T., Mechnik, V.A., Kolodnitsky, V.M., Kuttybayev, A., Muzapparova, A. Drilling inserts of the WC-Co-CrB2 system with increased mechanical properties. (2021) International Multidisciplinary Scientific GeoConference Surveying Geology and Mining Ecology Management, SGEM, 21 (1.1), 617–626. DOI: 10.5593/sgem2021/1.1/s06.111
32. Ratov B.T., Mechnik V.A., Gevorkyan S., Matijosius J., Kolodnitskyi V.M., Chishkala V.A., Kuzin N.O., Siemiatkowski Z., Rucki M. Influence of CrB2 additive on the morphology, structure, microhardness and fracture resistance of diamond composites based on WC–Co matrix. Materialia, 2022; 25: 101546. https://doi.org/10.1016/j.mtla.2022.101546
33. Mechnik V.A. Production of diamond–(Fe–Cu–Ni–Sn) composites with high wear resistance. Powder Metall. Met. Ceram. 2014; 52(9–10): 577–587.
34. Mechnik V.A., Bondarenko N.A., Kolodnitskyi V.M., Zakiev V.I., Zakiev I.M., Gevorkyan E.S., Kuzin N.O., Yakushenko O.S., Semak I. V. Comparative study of the mechanical and tribological characteristics of Fe–Cu–Ni–Sn composites with different CrB2 content under dry and wet friction. Journal of Superhard Materials 2021; 43(1): 52–64.
35. Han Y., Zhang S., Bai R., Zhou H., Su Z., Wu J., Wang J. Effect of nano-vanadium nitride on

microstructure and properties of sintered Fe–Cu-based diamond composites. Int. J. Refract. Met. Hard Mater. 2020; 91: 105256.

36. Mechnik V.A., Bondarenko N.A., Kuzin N.O., Gevorkian E.S. Influence of the addition of vanadium nitride on the structure and specifications of a diamond–(Fe–Cu–Ni–Sn) composite system. J. Frict. Wear. 2018; 39(2): 108–113.
37. Chen X., Du Y., Chung Y.W. Commentary on using H/E and H^3/E^2 as proxies for fracture toughness of hard coatings. Thin Solid Films 2019; 688: 137265.
38. Weaver J.C., Wang Q., Miserez A., Tantuccio A., Stromberg R., Bozhilov K.N., Maxwell P., Nay R., Heier S.T., DiMasi E., Kisailus D. Insight Analysis of an ultra hard magnetic biomineral in chiton radular teeth. Materials Today 2010; 13(1–2): 42–52.
39. Tokita M. Progress of Spark Plasma Sintering (SPS) Method, Systems. Ceramics Applications and Industrialization. Ceramics 2021; 4: 160–198. https://doi.org/10.3390/ceramics4020014
40. Stuer M., Bowen P., Zhao Z. Spark Plasma Sintering of Ceramics: From Modeling to Practice. Ceramics 2020; 3: 476–493. https://doi.org/10.3390/ceramics3040039
41. Gevorkyan E.S., Rucki M., Chishkala V.A., Kislitsa M.V., Siemiatkowski Z., Morozow D. Hot pressing of tungsten monocarbide nanopowder mixtures by electroconsolidation method. Journal of Machine Construction and Maintenance 2019; 113(2): 67–73.
42. Azevêdo H., Raimundo R., Silva D., Morais L., Macedo D., Cavalcante D., Gomes U. Microstructure and mechanical properties of Al2O3-WC-Co composites obtained by spark plasma sintering. International Journal of Refractory Metals and Hard Materials 2021; 94: 105408.
43. Dai W., Yue B., Chang S., Bai H., Liu B. Mechanical properties and microstructural characteristics of WC-bronze-based impregnated diamond composite reinforced by nano-NbC. Tribology International 2022; 174: 107777. https://doi.org/10.1016/j.triboint.2022.107777
44. Oliver W.C., Pharr G.M. Measurement of hardness and elastic modulus by instrumented indentation: advances in understanding and refinements to methodology. J. Mater. Res. 2004; 19(1): 3–20.
45. Mechnik V.A., Bondarenko N.A., Kolodnitskyi V.M., Zakiev V.I., Zakiev I.M., Ignatovich S.R., Dub S.N., Kuzin N.O. Formation of Fe-Cu-Ni-Sn-VN nanocrystalline matrix by vacuum hot pressing for diamond-containing composite. Mechanical and Tribological Properties. J. Superhard Mater. 2019; 41(6): 388−401.